Experimental characterization of rolled annealed copper film used in flexible printed circuit boards: Identification of the elastic-plastic and low-cycle fatigue behaviors

Gautier Girard, Marion Martiny, Sébastien Mercier

Experimental characterization of rolled annealed copper film used in flexible printed circuit boards: Identification of the elastic-plastic and low-cycle fatigue behaviors

Gautier Girard*, Marion Martiny, Sébastien Mercier

Université de Lorraine - CNRS - Arts et Métiers ParisTech, Laboratoire d'Etude des Microstructures et de Mécanique des Matériaux, 7 rue Félix Savart 57070 Metz, France

Abstract

The elastic-plastic and low-cycle fatigue behaviors of copper films are studied experimentally and identified for further simulation works. A rolled annealed copper grade is considered here, as it is often used in flexible printed circuit boards for its mechanical resistance to high elongations. During operation, the printed circuit board (PCB) will undergo various loadings, whether purely mechanical or environmental. These loadings can lead to the fracture of copper and thus to the disconnection of the electrical signal in the PCB. Copper has a low yield stress, so it undergoes easily plastic deformation. In the present work, a predominant kinematic hardening has been observed experimentally and modeled with the combined hardening model of Lemaitre-Chaboche. The fatigue behavior has been identified on cyclic loadings at different strain amplitudes. A Coffin-Manson model has been adopted to reproduce experimental data. Identified behaviors have been introduced in a numerical simulation of a flexible PCB under cyclic bending/reverse bending, in order to estimate its mechanical reliability.

Keywords: Copper film, Mechanical tests, Low-cycle fatigue, Elastic-plastic behavior, Kinematic hardening, Printed circuit boards

1. Introduction

The reliability of Printed Circuit Boards (PCB) has always been a subject of interest for manufacturers and consumers. As many industrial products are controlled by electronics, reliability concerns are shared in numerous industries such as space, aeronautics, automotive, defense or medical companies. A PCB is a multilayer, multi-material structure and its reliability mainly depends on the interactions and incompatibilities between the materials. During its lifetime, the PCB should withstand a large number of thermal cycles and each electrical connection should be preserved at any time. Prerequisites for lifetime predictions are at least a precise knowledge of the constitutive behavior of all materials involved and the definition of a failure criterion. For many applications, the lifetime of a PCB is limited by plasticity development generating low cycle fatigue. All these key ingredients are necessary to develop predictive finite element simulations of PCB structures. In the present study, the focus is made on copper, since it acts as the carrier of the electrical signal. The aim is to determine experimentally and to model the elastic-plastic and low-cycle fatigue behaviors of copper. As the mechanical response of copper is strongly related to the processing route, we select in the present paper a configuration valid for flexible PCB, with a rolled annealed copper layered on a polyimide substrate.

Note that researches are also conducted to propose new substrates for specific applications and there is a strong need to characterize these new materials. For instance, a previous work (Girard et al. [1]) concentrated on the orthotropic mechanical behavior of laminates for PCBs with high frequency space applications. For flexible PCBs, the thermal management inherited from the huge increase in power density needs the development of combination of materials to obtain larger thermal conductivity. Graphene film laminated with the polyimide substrate was proposed recently by Wang et al. [2].

To help manufacturers to satisfy the demand of consumers in terms of reliability, a continuous effort of research has been pursued during the last decades. It must be recognized that many authors focused on the thermo-mechanical response of rigid multilayer PCBs with a large number of plated through holes (PTHs). Mismatch in coefficients of thermal expansion of copper and dielectric materials, especially in the out-of plane direction, often leads to the occurrence of cracks in copper. In many articles, the reliability of PTHs is addressed by means of finite element simulations. Weinberg and Müller [3] considered a rigid PCB subjected to various thermal loadings. The copper behavior is assumed elastic-plastic with isotropic hardening. Void damage was triggered within copper path during plastic cycling. This damage mechanism was also adopted in Fellner et al. [4] who made a correlation between the evolution of the electrical resistance and the void volume fraction. The assumption of damage by void growth is not adopted in our work. Huang et al. [5] and Salahouelhadj et al. [6] considered flex-rigid PCBs with a central layer of polyimide material. From results on test vehicules facing standard thermal cycles, a failure criterion based on plastic strain increment (low-cycle fatigue model) was calibrated. Indeed, by monitoring the resistance evolution via an event detector, the number of cycles to failure was captured. For the FE simulations, the authors nevertheless adopted material parameters mostly taken from the literature. Note that in Salahouelhadj et al. [6], combined isotropic

*Corresponding author

Email address: gautier.girard@univ-lorraine.fr (Gautier Girard)

and kinematic hardening was taken into account, and identified from loading-unloading experiments on samples made of thick electrodeposited copper.

In these previous works, as tests are performed on PCBs with PTHs, local direct strain measurements are impossible, so the link between plastic strain and cycle to failure has to be done through a simulation of the PCB structure. To overcome this problem, authors have proposed to develop independent experiments to calibrate fatigue models. Merchant et al. [7, 8] worked on the low-cycle and high-cycle fatigue of copper foils with thickness in the range 12 to 35 µm. They studied the effects of the copper grade (electrodeposited, rolled, commercial grades), of the thickness, and of the annealing process on the fatigue life. All these factors were shown to have a strong impact on the fatigue life. The Coffin-Manson relationship (Coffin [9] and Manson [10]) was used here to relate the total strain amplitude in a cycle to the fatigue life. Note that the authors adopted the total strain amplitude in the Coffin-Manson law, instead of the accumulated plastic strain during the stabilized cycle, as the plastic behavior of copper was not identified. Watanabe et al. [11] designed an hourglass shaped specimen for evaluating the fatigue behavior of electrodeposited copper on an epoxy core. The proposed method allowed the application of tensile-compressive loadings on a copper film similar to the one found in a PTH and the direct assessment of the fatigue behavior of electrodeposited copper. Su et al. [12] developed a specific specimen made of a 3 mm thick PCB layered on the external surfaces by electrodeposited copper. Four point bending tests were performed to calibrate the Coffin-Manson model. The predictions of the failure criterion together with FE simulations were able to reproduce experimental trends observed on test vehicules. For flexible electronics, one can mention the work of Lee et al. [13] who investigated the stretchability and fatigue failure of copper deposited on a polyimide substrate. Tensile and cyclic bending tests on three different samples (non-annealed, 150 °C annealed and 300 °C annealed) have been performed. Annealed samples are shown to have a larger ductility and for the same applied strain during a tensile loading, their resistivity increase was smaller than in non-annealed samples. In addition, during cyclic bending, annealed samples showed a larger resistivity increase after the same number of applied cycles. The authors related these findings to the lower yield strength of annealed samples (having large grains), promoting the dislocation motion and the occurrence of cracks. Beck et al. [14] developed flexural fatigue tests, according to standard IPC-TM-650 Method 2.4.3.1. They compared the flexural fatigue life of bare copper and copper/polyimide samples. The role of the copper thickness and width of the copper path was investigated.

An additional important prerequisite is to capture the cyclic elastic-plastic response of copper. In some cases, the mechanical behavior of copper for PCB applications was assumed as elastic-plastic with isotropic hardening described by a linear relationship (Su et al. [12]) or a power law (Weinberg and Müller [3]). In some studies, the hardening of copper films was identified using monotonic loadings (Xiang et al. [15], Dudek et al. [16]). Such assumption limits the prediction capabilities of FE simulations, especially for cyclic loadings. During thermal or mechanical cycles, copper exhibits a significant kinematic hardening. Reproducing in an homogeneous independent experiment a stress-strain path representative of a situation experienced by copper during the PCB lifetime is challenging. Indeed, imposing tension/compression loadings to a thin film is not straightforward. Thus, Kraft et al. [17, 18], Ono et al. [19], Mönig et al. [20] proposed different methods to apply cyclic loadings on the copper film. The method which is often chosen (and will be adopted in the present work) consists in using an elastic compliant substrate on which the copper film is deposited. During uniaxial tension loading/unloading, copper film is facing tension-compression cycles. Owing to the low yield stress of the copper grade used for PCBs, it will deform plastically while the substrate remains elastic. A conclusion of these studies was the strong dependency of the mechanical response and of the low cycle fatigue to the film thickness, grain size and processing route. Wimmer et al. [21] also showed a grain size effect on the yield stress, the Young's modulus and the number of cycles to failure. Fellner et al. [22] performed similar experiments on a composite sample made of copper and glass fiber-epoxy resin material. Tests were performed at different temperatures and overall cyclic forces. The experimental stress-strain response was modeled using the Lemaitre and Chaboche work [23, 24] with a combined isotropic and kinematic hardening. Fellner et al. [25] validated the previous approach by developing a non isothermal experiments with a bi-material sample consisting of a thin copper film sputtered onto a silicon substrate.

The behavior of copper has been widely studied in literature and numerous studies showed the difference between the behavior of bulk copper and copper films. Indeed, at small scales, the size of microstructural features (i.e. grains) can be of the order of magnitude of the film thickness. Thus, mechanisms occurring during deformation are modified when compared to bulk copper. A detailed literature overview on the subject of size effects was realized by Simons et al. [26], who showed a strong effect of copper thickness on the fracture strain, going from 20 % to 0.2 % when the sample thickness is reduced from 150 µm to 10 µm. The effect of heat treatment was also shown on rolled copper: the fracture strain of a 10 µm thick copper foil can increase from 0.2 % to 15 % with a salient heat treatment. From all these studies, it is clear that consistent information is needed in order to develop predictive simulations of PCB structures. The only possibility to reach that goal is to characterize the particular film used in the PCB structure of interest.

In the present work, as already mentioned, we focus on a configuration valid for flexible electronics (17.5 µm thick rolled annealed copper layered on polyimide substrate). It has also been seen that such configuration is also adopted for flex-rigid PCB. Our goal is to identify the cyclic elastic-plastic response of this copper grade and provide information on low cycle fatigue. The Lemaitre-Chaboche combined hardening model is used to reproduce the experimental response of copper. From the original fatigue experimental setup, parameters of the Coffin-Manson law are identified for this copper grade. Finally, the response of a flexible PCB structure under a cyclic bending

loading is studied by numerical simulation, adopting the material parameters previously identified. The method proposed here can be applied to any copper film used in a PCB (for example electrodeposited copper). Results are provided for room temperature but a similar work could also be done for different temperatures or non-isothermal conditions.

2. Experimental setups and measurements

As discussed in the introduction part, predictive simulations require precise material constitutive law and failure criterion. In this section, cyclic loading-unloading and fatigue tests are performed in order to describe the elastic-plastic and the low-cycle fatigue responses of a rolled-annealed copper used in the PCB industry.

2.1. Elastic-plastic response

As a film can not support compression because of buckling, it has been proposed in the literature [17, 18] to develop a composite specimen made of film and substrate, as shown in Fig. 1a. The substrate is compliant so that its elastic domain in terms of strain is larger than the one of copper. During the considered tensile loading, the substrate remains elastic while copper undergoes plastic deformation. During unloading, the substrate will push copper in compression. The drawback of this method is that the copper behavior is not directly assessed. Only the overall response of the sample (substrate with copper) is measured. An inverse analysis is thus necessary to get the behavior of copper. To obtain reliable data on copper from the inverse analysis, the proportions of each material within the sample have to be carefully chosen. As our goal is to study a configuration which is often adopted in flexible PCBs, a commercial panel with a $17.5\,\mu\mathrm{m}$ thick copper film and a $75\,\mu\mathrm{m}$ thick polyimide substrate are considered. Owing to the process tolerance, a precise measurement of the thicknesses is made. It is found that the copper layer (resp. polyimide core) is $18.15\,\mu\mathrm{m}$ (resp $71.4\,\mu\mathrm{m}$) thick. From the panel, samples have been manufactured, see Fig. 1a. By etching copper in the gauge section, specimens with substrate only are obtained, see Fig. 1b. The two samples have been tested in the tensile machine INSTRON E3000. The crosshead speed is set to $2\,\mathrm{mm\,min^{-1}}$ for all tests considered in the present paper.

Samples of Fig. 1b with three orientations (0°, 45° and 90°) have been tested in order to validate the in-plane isotropy of the substrate. A speckle is created on the specimen surface with spray-paint so that strains are measured by Digital Image Correlation (DIC). For each direction, one sample has been tested up to $200\,\mathrm{N}$ to determine the elastic limit of the substrate. The same elastic limit of approximately $65\,\mathrm{MPa}$ has been found for each direction. The corresponding longitudinal strain is $\varepsilon_{xx} = 0.01$. Subsequently three tests for each orientation have been performed to measure the elastic modulus. DIC results show homogeneous strains in the working area (gauge section) of the samples. In-plane strain components are obtained by averaging the values on this area. With the crosshead velocity of $2\,\mathrm{mm\,min^{-1}}$, the longitudinal strain rate

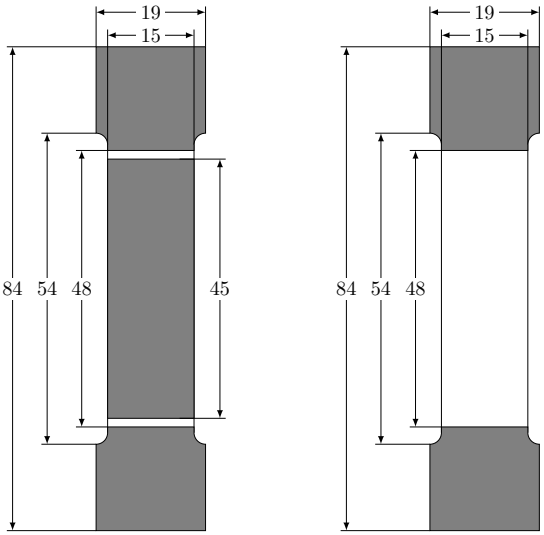

(a) Test specimen made of substrate with copper on both sides.

(b) Test specimen for the identification of the substrate behavior.

Figure 1: Layout of the specimens used for the identification of the elastic-plastic behavior of copper and the elastic behavior of the substrate.

is close to $5 \times 10^{-4}\,\mathrm{s^{-1}}$ during the loading. From the stress-strain response of the substrate for the three selected orientations, it is found that the Young's modulus is varying slightly from $8.4\,\mathrm{GPa}$ at 0° to $7.8\,\mathrm{GPa}$ at 90°, see Table 1. Based on the strain components ε_{xx} and ε_{yy} captured by DIC, the Poisson's ratio is measured and is close to 0.28. From results presented in Table 1, we assume that the substrate has an isotropic elastic behavior (at least in the plane) for the considered strain amplitude. The average Young's modulus is adopted in the following.

Direction	0°	45°	90°
Young's modulus [GPa]	8.40	8.02	7.84
Poisson's ratio [-]	0.288	0.285	0.269

Table 1: Measured elastic moduli for the substrate with different orientations at room temperature.

For the substrate to remain elastic, the maximum longitudinal strain during loading should not exceed $\varepsilon_{xx} < 0.01$. Such strain amplitude corresponds to the range that a PCB can face in operation. Samples of Fig. 1a are subjected to 100 uniaxial tensile cycles with a force varying between $10\,\mathrm{N}$ and $130\,\mathrm{N}$. The crosshead velocity is still set to $2\,\mathrm{mm\,min^{-1}}$, as for tests on the substrate. The maximum force value generates approximately $1\,\%$ longitudinal strain. The lower load value is positive to prevent buckling of the sample. DIC is still used to measure strains on the copper surface and the force is measured by an Instron dynamic load cell of $\pm 1\,\mathrm{kN}$ capacity. The longitudinal strain rate during loadings was measured to $5 \times 10^{-4}\,\mathrm{s^{-1}}$.

The experimental response of the substrate + copper sample at orientation 0° is shown on Fig. 2 where the first, 10^{th}, 50^{th} and 100^{th} cycles are plotted. One can note that the cyclic

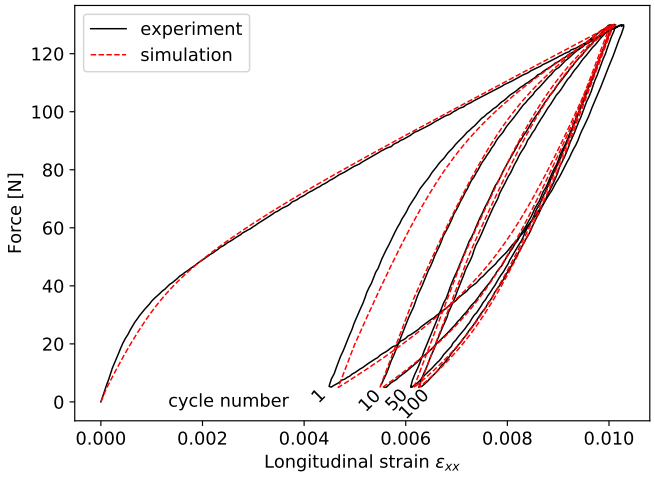

Figure 2: Evolution of the overall force versus longitudinal strain. Comparison of experimental data and simulated cyclic response after identification of the copper behavior. The first, 10^{th}, 50^{th} and 100^{th} cycles are plotted. The assembly of a polyimide core and rolled annealed copper is considered.

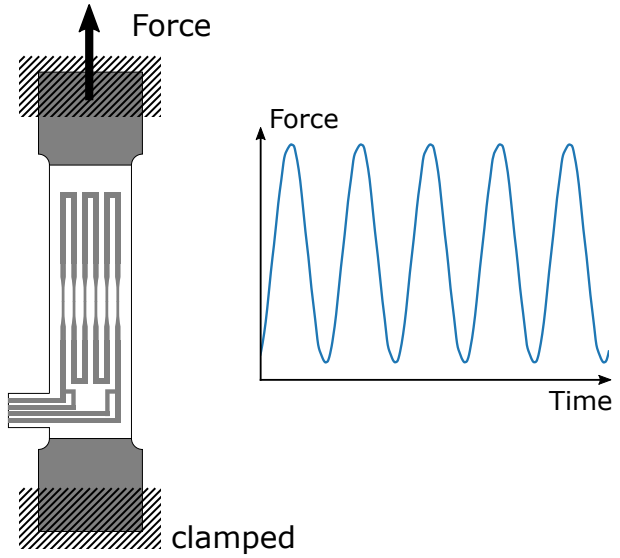

Figure 3: Fatigue test specimen with the same daisy chain on each side. The daisy chain is made of 6 traces aligned in the loading direction. The daisy chain is connected to a milliohmmeter via the plug. A four-terminal sensing measuring technique is adopted here to measure the electrical resistance.

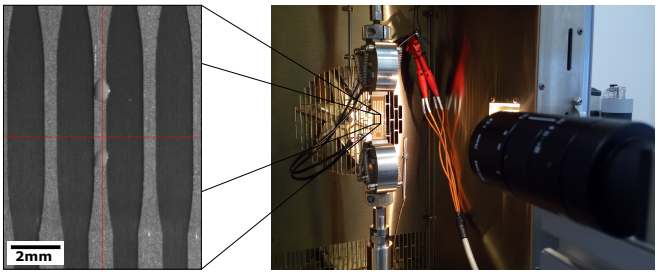

Figure 4: Experimental setup for fatigue characterization of the copper film. The longitudinal strain is obtained via the monitoring of the distance between the two dots present in the central part of the specimen (two points tracking system). The electrical resistance of the daisy chain is monitored in real time, together with the longitudinal strain and the force.

response is not completely stabilized after 100 cycles. Tests have been performed for two orientations $0°$ and $90°$ and the overall response during loadings and unloadings presents little differences. A clear hysteresis loop is present close to the stabilization and is due to kinematic hardening in copper.

Next, the low cycle fatigue of the copper foil is investigated.

2.2. *Fatigue characterization*

The same method as in Section 3.1 is used to apply tensile-compressive loadings to copper, i.e. the copper is present on both side of the same compliant substrate. Nevertheless, to detect the failure of copper during loading, a specific sample seen in Fig. 3 has been designed. Note that this sample is different from the one proposed by the Institute for Interconnecting and Packaging Electronic Circuits via the IPC TM-650 2.4.3.1 standard [27] to analyze the fatigue life of copper traces during bending loading. The same copper path is present on both sides of the sample. Similarly to a strain gauge, 6 copper traces are aligned in the loading direction. It is seen in Fig. 3 that the central section of each trace is thinned. This width reduction follows the shape of a flat dogbone specimen. In the present case, the 6 copper traces have a width of 1 mm except in the gauge section where the width is reduced to 0.5 mm. With the present configuration, it is expected that failures will be observed in the gauge cross-section. Even with the present design, capturing copper failure during testing is not obvious. The idea is thus to measure the electrical resistance of the daisy chain during the experiment in order to detect the rise of the resistance, signature of a failure in one of the copper traces. This method is widely used in the literature, see for example Lee et al. [13] or Merchant et al. [8].

A milliohmmeter (Burster, resistomat 2329) has been used to monitor the electrical resistance in the copper path, forming a daisy chain. Four-terminal sensing measuring technique is used. A plug permits the connection of the sample to the milliohmmeter. The electrical resistance of the daisy chain is registered together with the other useful quantities (time, strain, force, temperature) so that all data are synchronized.

A sinusoidal force is applied to the specimen at a frequency of $1\,\mathrm{Hz}$. Since samples are thin and elongated, the load should not be negative to avoid specimen buckling; the lower bound of the force is always set to $10\,\mathrm{N}$. The longitudinal strain is recorded during the experiment and is measured by a two-point tracking method. Two small dots (of diameter $0.5\,\mathrm{mm}$) are drawn in the middle of one gauge cross-section (see Fig. 4). A camera with a macro lens records the experiment (camera IDS USB 3 uEye CP, approximately 500 frames/s). A dedicated program developed by ProViSys company detects the two dots and measures the distance between them for each frame. The experimental setup is shown on Fig. 4. The longitudinal strain

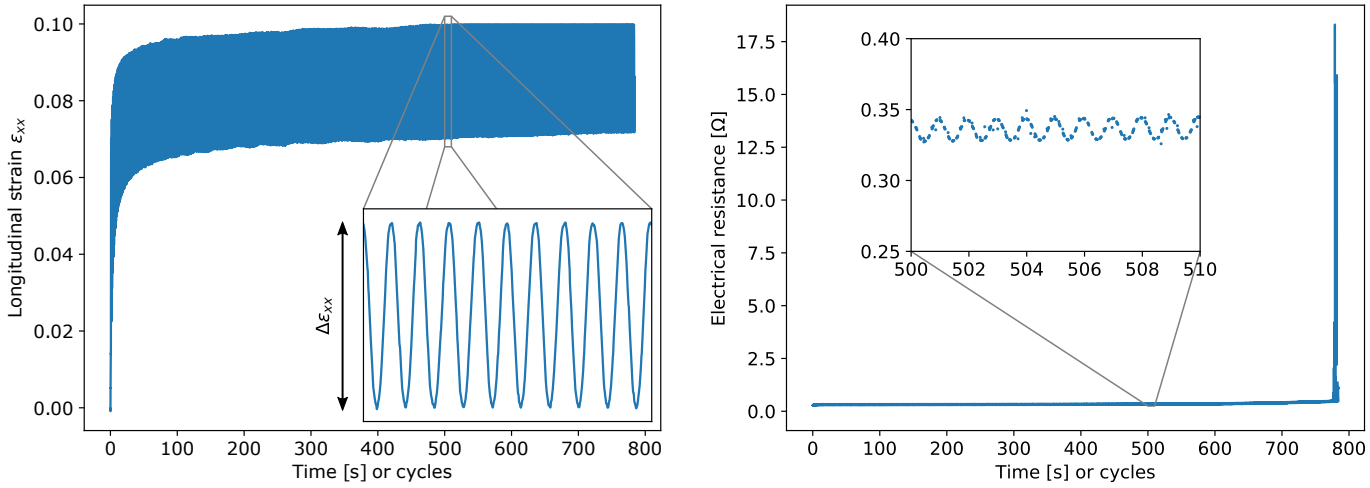

(a) (b)

Figure 5: Experimental measurements of (a) the longitudinal strain (b) the electrical resistance of the daisy chain during the cyclic loading. A stabilized strain amplitude is observed after a few tens of cycles. Note that tests are performed at a frequency of 1 Hz. Here, results are depicted with a maximum force equal to 260 N. After 780 cycles, the first event is detected meaning that one copper trace is broken in the front side of the sample. An oscillating evolution of the resistance (with limited amplitude) is observed during the test, at the frequency of the applied cycles. This fluctuation corresponds to the change of resistance associated to the cyclic deformation of the copper. Rolled annealed copper is considered.

is computed in real time and registered. Fig. 5a shows the measured longitudinal strain during an experiment. Here, the maximum force is set to $F_{max} = 260\,\mathrm{N}$. The strain amplitude is observed to stabilize after a few tens of cycles.

The electrical resistance is measured only on one face of the sample. The value is representative of the resistance of the whole daisy chain, see Fig. 5b. In the zoomed part of Fig. 5b is presented also the resistance evolution due to cyclic straining before failure. The associated resistance change is limited. Once one of the six traces breaks, the measured electrical resistance suddenly increases, as seen on Fig. 5b. The test is then paused and all twelve copper traces (on both sides of the sample) are tested one by one with an ohmmeter. To do so, the specimen is still under tension (the mean force is applied to the sample to keep cracks in copper open). The broken trace is easily localized, since its resistance is significantly higher, and the number of cycles corresponding to its failure is recorded. Note that one or several broken traces may exist on the rear side as well, since the electrical resistance is not monitored there. In our tests, in some cases, one trace was already broken. Those already broken traces are marked by a dash "-" on Figs. 6 and 9a. The test is then continued by series of additional cycles. The number of cycles in a series corresponds to 5 % of the cycle number at the first failure event. All traces are tested after each series. The test is continued until all traces fail. The number of cycles to failure of each trace is captured. During these subsequent series, more than one trace can fail, thus the number of dots on Figs. 6 and 9a can be smaller than twelve (total number of traces on a specimen). With one sample, one can thus obtain twelve events, corresponding to the failure of each individual trace.

The longitudinal strain is recorded during all the process, and it has been checked that the strain amplitude remains almost unchanged after the failure of a copper trace. Indeed, the failure of all twelve traces led to a slight increase of the strain amplitude, less than 5 % for all amplitudes tested. Indeed, for this specimen, the mechanical response of the sample is mostly driven by the substrate.

Subsequently, different force amplitudes have been considered. The lower force is still 10 N. The upper force for the cycle is varying from 100 N to 260 N. It is observed for all tests that the total strain amplitude is stabilized after a few tens of cycles. In Fig. 5a, with a maximum force of 260 N, the strain amplitude was stabilized after 100 cycles. Therefore, it can be reasonably considered that copper traces are subjected during tests to a well defined strain amplitude. From the different force amplitudes, the number of cycles to failure of each trace is linked to the total longitudinal strain amplitude $\Delta\varepsilon_{xx}$ measured on the copper trace (Fig. 6). As expected, as the maximum force increases, the strain amplitude $\Delta\varepsilon_{xx}$ becomes larger and the mean fatigue life of all copper traces is reduced. Note that for the considered strain amplitudes, copper will experience plasticity during cycles. Therefore, before evaluation of the accumulated plastic strain increment during stabilized cycles and identification of the parameters of the Coffin-Manson law, one needs to propose a constitutive model for the cyclic plasticity of copper, based on results of Fig. 2.

Note that all results presented in this section are valid for the particular structure studied here: a commercial rolled annealed copper supported by a polyimide substrate. Knowing the mechanical response of other copper grades (like plated copper) would require similar experiments.

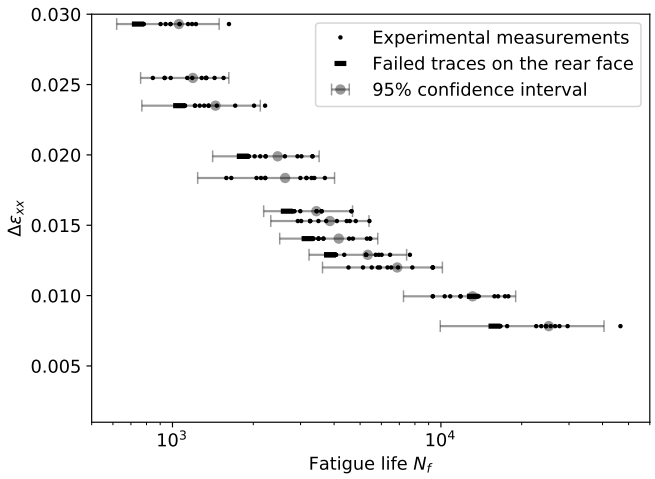

Figure 6: Number of cycles to failure N_f related to the strain increment $\Delta\varepsilon_{xx}$. For each $\Delta\varepsilon_{xx}$, twelve events have been detected. The means and error bars for failure are plotted for each sample. Each error bar is constructed using a 95 % confidence interval. The dash present for some strain amplitudes means that a copper trace on the rear face was also broken when the first trace failed on the front face of the specimen. Rolled annealed copper is considered.

3. Modeling and results

3.1. Elastic-plastic behavior of copper

To model the combined isotropic and kinematic hardening of copper observed in Fig. 2, the Lemaitre-Chaboche model [24] is adopted. The main equations are presented next. The total strain rate tensor $\dot{\boldsymbol{\varepsilon}}$ is the sum of elastic $\dot{\boldsymbol{\varepsilon}}^{\mathrm{e}}$ and plastic strain rate $\dot{\boldsymbol{\varepsilon}}^{\mathrm{p}}$ tensors:

$$\dot{\boldsymbol{\varepsilon}} = \dot{\boldsymbol{\varepsilon}}^{\mathrm{e}} + \dot{\boldsymbol{\varepsilon}}^{\mathrm{p}} \tag{1}$$

The elastic behavior of copper is given by the Hooke's law:

$$\dot{\boldsymbol{\sigma}} = \mathbf{A}^{\mathrm{e}} : \dot{\boldsymbol{\varepsilon}}^{\mathrm{e}} \tag{2}$$

where $\mathbf{A}^{\mathrm{e}}$ is the fourth order elastic stiffness tensor. The tensorial operator ":" is the double contracted product operator. In the present paper, we assume that the elastic response of copper is isotropic. Only E^{cu} and ν^{cu} are necessary to describe the elastic behavior of copper.

A J_2 flow rule is adopted so that the plastic strain rate tensor $\dot{\boldsymbol{\varepsilon}}^{\mathrm{p}}$ is related to the deviator of the Cauchy stress tensor $\boldsymbol{s}$ and the backstress tensor $\boldsymbol{X}$ by:

$$\dot{\boldsymbol{\varepsilon}}^{\mathrm{p}} = \frac{3}{2}\dot{p}\frac{\boldsymbol{s}-\boldsymbol{X}}{J_2(\boldsymbol{\sigma}-\boldsymbol{X})} \tag{3}$$

where $J_2(\boldsymbol{\sigma}-\boldsymbol{X}) = \sqrt{\frac{3}{2}(\boldsymbol{s}-\boldsymbol{X}):(\boldsymbol{s}-\boldsymbol{X})}$ is the effective stress and $\dot{p} = \sqrt{\frac{2}{3}\dot{\boldsymbol{\varepsilon}}^{\mathrm{p}}:\dot{\boldsymbol{\varepsilon}}^{\mathrm{p}}}$ is the effective plastic strain rate. The yield surface is defined by:

$$f_y = J_2(\boldsymbol{\sigma}-\boldsymbol{X}) - R(p) - \sigma_{\mathrm{o}} \tag{4}$$

During plastic loading, $f_y = 0$. σ_{o} is the initial yield stress. $p = \int \dot{p}\, dt$ is the accumulated platic strain. R is representative of isotropic hardening. Its evolution law is given by:

$$\dot{R} = b(Q-R)\dot{p} \tag{5}$$

b and Q are material parameters. Q is the saturation value and b is the saturation rate of the isotropic hardening variable. By integration of Eq. (5) with $R(p=0)=0$, the isotropic hardening of copper is described by the following relation: $R(p) = Q(1-e^{-bp})$.

In the Lemaitre-Chaboche model, the backstress is made of several components: $\boldsymbol{X} = \sum_{i=1}^{N_{LC}} \boldsymbol{X}_i$, with N_{LC} the total number of components. The evolution law of each component of the backstress is given by:

$$\dot{\boldsymbol{X}}_i = \frac{3}{2}C_i\dot{\boldsymbol{\varepsilon}}^{\mathrm{p}} - \gamma_i\boldsymbol{X}_i\dot{p} \tag{6}$$

where C_i and γ_i are material parameters.

In the following, the value $N_{LC} = 3$ is adopted. As a consequence, eleven parameters (E^{cu}, ν^{cu}, σ_{o}, C_1, γ_1, C_2, γ_2, C_3, γ_3, Q and b) have to be identified. They will be evaluated by combining Finite Element calculations and optimization procedure. A Finite Element model of the substrate-copper sample depicted in Fig. 1a is built. The simulated structure is subjected to the same loadings (in terms of overall force) as in the experiment and the predicted strains are compared to the measured experimental strains. A cost function f_{cost} defined as:

$$f_{cost} = \frac{1}{N}\sum_{i}^{N}\left(\varepsilon^i_{xx,exp} - \varepsilon^i_{xx,sim}\right)^2 \tag{7}$$

is comparing the simulated $\varepsilon^i_{xx,sim}$ and measured $\varepsilon^i_{xx,exp}$ strains for any registered data. In our case, $N = 19000$ for 100 cycles. Note that only the longitudinal strains are present in the cost function. Nevertheless, as the sample is subjected to uniaxial tensile force and made of two different materials, transversal strains develop as the result of the interaction between the two materials. This cost function is minimized by optimizing the material parameters of the Lemaitre-Chaboche model with a Nelder-Mead algorithm. The algorithm is modified to ensure that no negative values are used for the material parameters (no cyclic softening was observed during the experimental tests).

The initial conditions for the optimization are taken from the work of Salahouelhadj et al. [6]. The algorithm stops when the cost function has reached a plateau value (i.e. the cost function value does not decrease for 40 iterations). Thus a set of parameters involved in the elastic-plastic constitutive law of copper is found. To check the robustness of the solution, different initial sets of parameters (randomly chosen) have been additionally tested and have led to the same converged solution. The set of parameters found is presented in Table 2. The simulated mechanical response of the sample is shown together with the experimental response on Fig. 2 for cycles number 1, 10, 50 and 100. A very good agreement is reached.

The mechanical response of copper derived from the FE simulations is displayed in Fig. 7a. One observes that the dif-

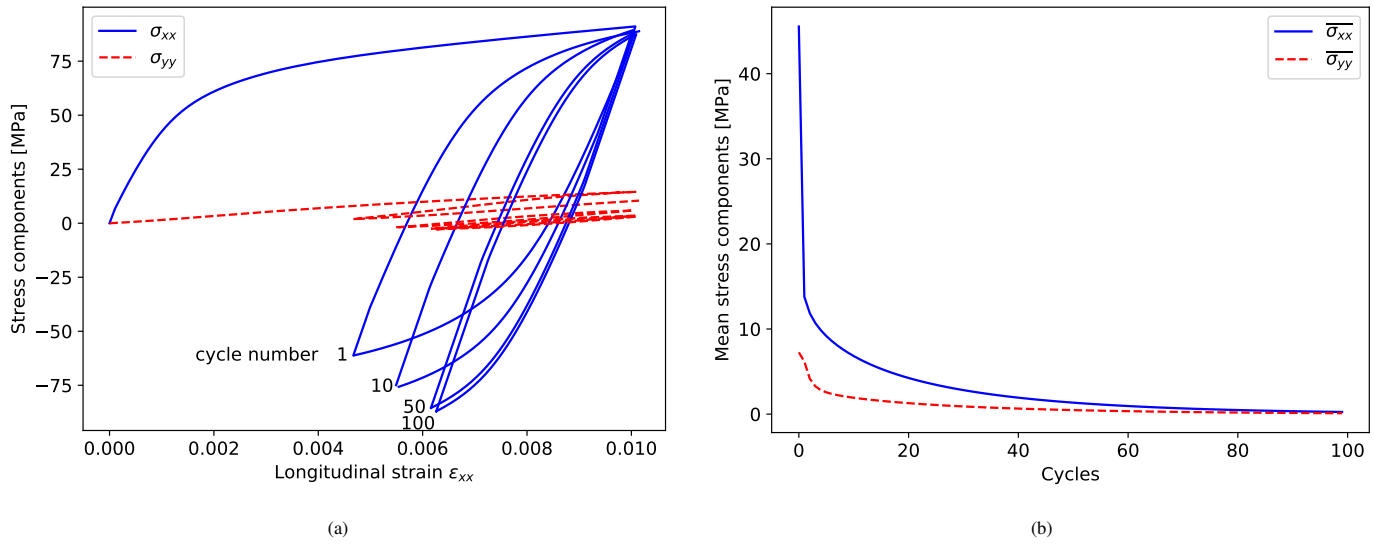

(a) (b)

Figure 7: Response of the rolled annealed copper on a flexible substrate when subjected to cyclic loadings. (a) Longitudinal and transversal stress components versus longitudinal strain. The first, 10$^{\text{th}}$, 50$^{\text{th}}$ and 100$^{\text{th}}$ cycles are plotted. (b) Evolution of the mean stress as a function of the number of cycles, for the two components σ_{xx} and σ_{yy}.

ference in Poisson's ratios between the copper film and the substrate as well as plasticity development in copper lead to non-vanishing transversal stress. After the first loading, the transversal stress σ_{yy} reaches a value of 14 MPa, while the longitudinal stress σ_{xx} is around 91 MPa. During the first loading, the value of σ_{yy} corresponds to 15 % of σ_{xx}, which is not negligible. After 100 cycles, the maximum value of the transversal stress σ_{yy} reaches only 3 MPa, corresponding only to 3 % of σ_{xx} value.

For each cycle, the mean stress of component i is defined as:

$$\overline{\sigma_i} = \frac{\sigma_i^M + \sigma_i^m}{2} \tag{8}$$

with σ_i^M (resp. σ_i^m) the maximum (resp. minimum) value of the stress component i during the cycle. Fig. 7b shows that for both directions x and y, the mean stress is slowly approaching zero as the number of cycle increases. The transversal stresses are often neglected in the literature when analyzing the response of substrate-metal sample [28]. It is also important to mention that a PCB is made of several copper grades. The rolled annealed copper studied in this work shows a limited yield stress, when compared to electrodeposited copper. Indeed, the longitudinal stress faced by such copper grade during uniaxial tension will reach 90 MPa for a longitudinal strain of 0.01. For an electrodeposited copper, the longitudinal stress reaches 260 MPa for the same strain magnitude, see Salahouelhadj et al. [6].

3.2. *Identification of the Coffin-Manson model*

It has been seen in Fig. 6 that the total longitudinal strain amplitude $\Delta\varepsilon_{xx}$ during fatigue tests is large so copper develops low-cycle fatigue. It is known that the fatigue life is controlled by the intensity of the plastic flow during the cycles. To determine the number of cycles to failure during low cycle fatigue, we propose to adopt the Coffin-Manson relation [10]:

$$N_f = \frac{1}{2}\left(\frac{\Delta p}{2\varepsilon_f}\right)^{1/c} \tag{9}$$

which links the accumulated plastic strain increment Δp during the stabilized cycle to the fatigue life N_f. c and ε_f are parameters to be determined for the considered copper grade. This equation is usually adopted for fatigue of copper in printed circuit boards [3, 5, 6, 11]. Merchant et al. [7, 8] used the same relation, except they considered the total strain amplitude and not the accumulated plastic strain amplitude. It is important to mention that the knowledge of the fatigue life as a function of the longitudinal strain amplitude can only be used for uniaxial tension. For other mechanical loadings, the strain tensor can have a general form and only the accumulated plastic strain increment is meaningful. Note that other relationships have been proposed in the literature [29] and could have been selected. In our paper, the main challenge is to obtain reliable prediction of the accumulated plastic strain increment, and not the selection of one particular law. When the material remains mainly in the elastic domain, the number of cycles to failure is higher (more than a few thousands), other relations are to be used to describe the high cycle fatigue (HCF) regime.

As the elastic-plastic behavior has been identified for the studied copper in Section 3.1, a Finite Element simulation of the sample defined in Fig. 3 is carried out in order to determine the plastic strain accumulated during cycles. In the simulations, the substrate is assumed to remain elastic. This assumption is valid when the longitudinal strain remains lower than 1 %. For larger strains, this assumption is questionable. However, it has been seen in Section 3.1 that during cycles, the transversal stress component σ_{yy} in copper was limited and was decreasing with cycles. This may not be true for large strain amplitudes, but it may be reasonable to consider that for the

Parameter	E^{cu} [GPa]	ν^{cu} [-]	k [MPa]	C_1 [GPa]	γ_1 [-]	C_2 [GPa]	γ_2 [-]	C_3 [GPa]	γ_3 [-]	Q [MPa]	b [-]
Value	69.2	0.36	5.28	139	3977	23.9	877	1.59	13.98	30.1	15.5

Table 2: Identified parameters for the elastic-plastic behavior of the considered rolled annealed copper. Here the Lemaitre-Chaboche model [24] is adopted. The backstress is split into three components.

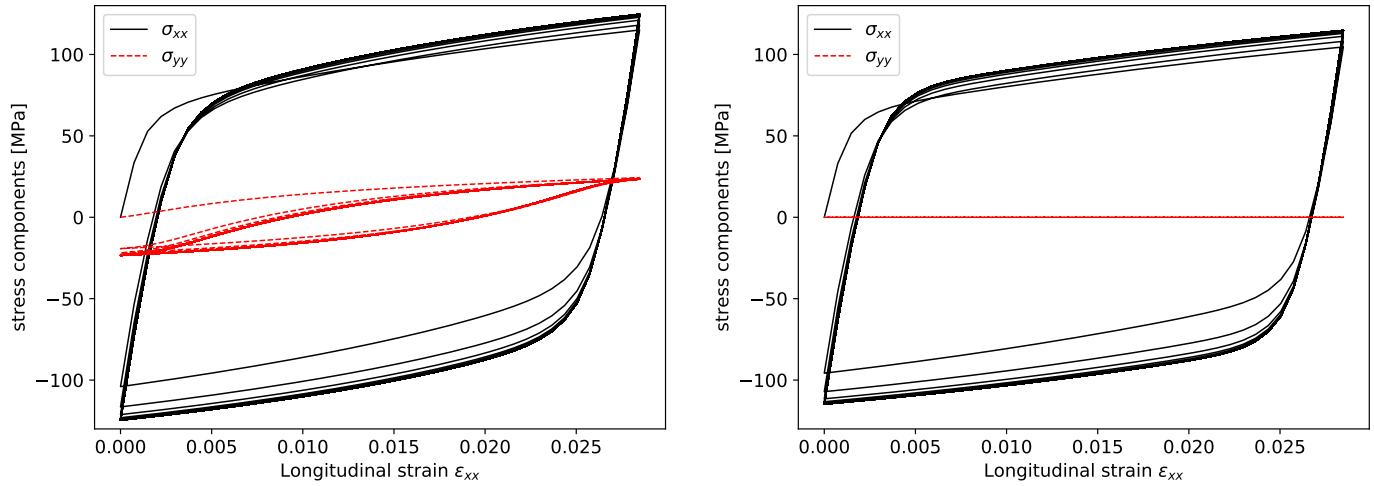

Figure 8: Results of cyclic simulation of (a) copper on an elastic substrate and (b) a copper foil. The stress components σ_{xx} and σ_{yy} in copper are shown. Both samples have been subjected to the same mechanical loading: 50 cycles with a longitudinal strain amplitude $\Delta\varepsilon_{xx} = 0.029$. The copper response stabilizes after only a few cycles. Rolled annealed copper is considered.

considered tests, the copper trace is facing an almost uniaxial loading after a few cycles of accommodation. Thus, the behavior of the substrate may not play a significant role in the stress development in the copper film. The substrate is only a support for applying tension-compression to the copper film.

In order to investigate the role of the substrate on the plasticity development in copper foil for a given strain amplitude, two series of FE simulations have been compared. The first simulation represents the copper foil on the elastic substrate and the second one considers the copper foil alone. Both numerical models are subjected to the same measured total strain amplitude. In this series of calculations, the longitudinal strain is assumed to vary cyclically from 0 to $\Delta\varepsilon_{xx}$. We present here the comparison for the largest longitudinal strain amplitude considered in the present work $\Delta\varepsilon_{xx} = 0.029$. Fig. 8 depicts the evolution of the stress components σ_{xx} and σ_{yy} versus longitudinal strain ε_{xx}. Fig. 8a corresponds to the configuration where copper is layered on the elastic substrate. Due to mismatch in mechanical properties, a non-zero σ_{yy} is present with a relative small amplitude when compared to σ_{xx}. Fig. 8b shows the response of copper alone, where of course $\sigma_{yy} = 0$. For this selected strain amplitude, the relative difference in Δp (accumulated plastic strain increment during a stabilized cycle) is finally less than $1\,\%$ between the two simulations. Considering either the copper alone or the configuration of copper on the elastic substrate leads to the same value of the accumulated plastic strain increment $\Delta p = 0.0552$. Note that Δp is computed over a full cycle, whereas $\Delta\varepsilon_{xx}$ corresponds to the amplitude of a reversal. Indeed, plasticity is accumulated during the first stage of the cycle where the strain is increasing and also during the second stage, when the strain is decreasing. Therefore, it is observed that Δp is almost equal to $2\Delta\varepsilon_{xx}$. Further information will be provided in Fig. 9b.

For each test, a FE simulation is performed with the corresponding stabilized total longitudinal strain amplitude $\Delta\varepsilon_{xx}$. The corresponding accumulated plastic strain increment is determined. Fig. 9a presents half the accumulated plastic strain increment $\Delta p/2$ against the number of cycles to failure N_f. The parameters of the Coffin-Manson equation (9) have been fitted to the fatigue data experimentally measured. The Levenberg-Marquardt algorithm is used to minimize the difference between predictions and data. The values of the parameters can be found in Table 3. Fig. 9a and Fig. 6 provide similar results, except that in Fig. 6, the longitudinal strain amplitude accounts for elastic and plastic parts. As the strain amplitude increases, the proportion of plastic strain in the total strain increases. Fig. 9b presents the ratio $(\Delta p/2)/\Delta\varepsilon_{xx}$ as a function of $\Delta\varepsilon_{xx}$. This ratio tends towards one for large $\Delta\varepsilon_{xx}$. On the contrary, as $\Delta\varepsilon_{xx}$ decreases, the intensity of the plastic flow is reduced and the number of cycles to failure becomes larger. It is well known that for HCF (a situation not considered here), this ratio must be close to zero. This trend is clearly observed in Fig. 9b.

The number of cycles to failure for this copper grade is rel-

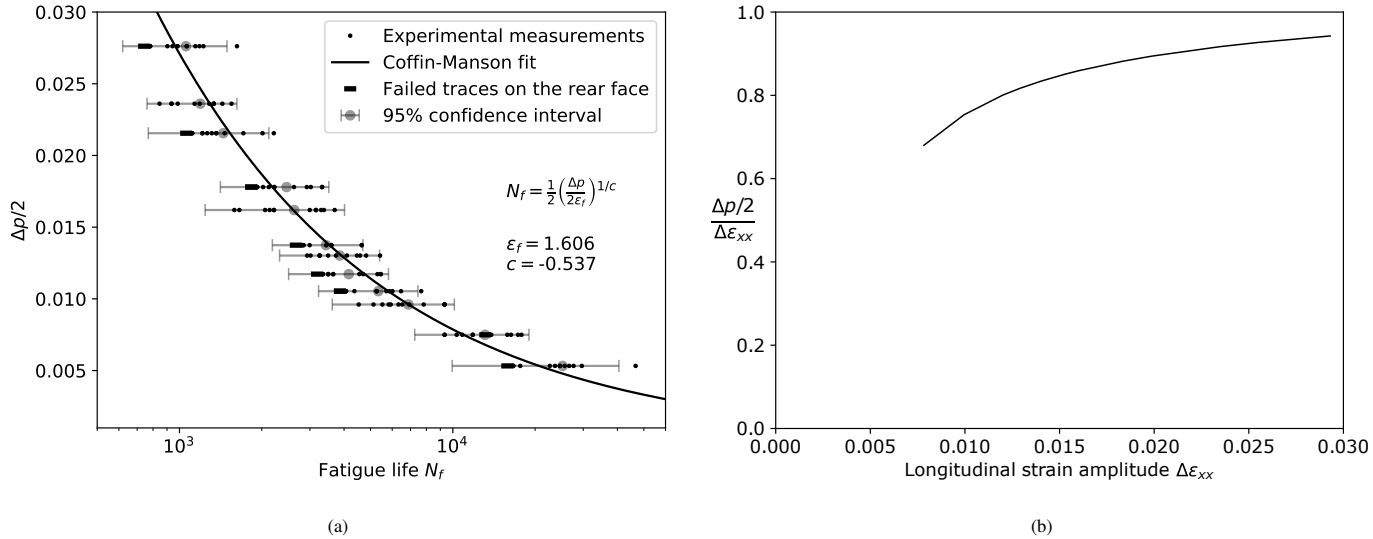

(a) (b)

Figure 9: Fatigue results: (a) Number of cycles to failure N_f versus half the accumulated plastic strain increment $\Delta p/2$. The values for the twelve traces are plotted with the corresponding means and error bars for each sample. Each error bar is constructed using a 95 % confidence interval. The fitted Coffin-Manson model reproduces the trend accurately. (b) Evolution of the ratio half the accumulated plastic strain during a stabilized cycle $\Delta p/2$ over the total longitudinal strain $\Delta \varepsilon_{xx}$ in the range of studied strain amplitudes. Rolled annealed copper is considered.

atively large when compared to the expected number of cycles to failure of multilayer printed circuit boards. This is not contradictory. Indeed, in multilayer PCBs, cracks are often observed in plated through holes (PTH), which are coated by electrodeposited copper. Weinberg and Müller [3] have worked on PTHs and adopted the following Coffin-Manson parameters: $\varepsilon_f = 0.2$ and c between -0.5 and -0.7. But as reported by Huang et al. [5], the electrodeposited copper shows a reduced fatigue life when compared to rolled annealed copper investigated in the present paper. As often used for flexible PCBs, the rolled annealed copper can be subjected to large deformation in operation and is more prone to withstand them. The different microstructures induced by the processing routes explain the difference in both elastic-plastic response and the fatigue behavior.

The results presented here are obtained at 1 Hz. A second frequency has been considered: 4 Hz. Let us consider cycles with oscillatory force between 10 N and 140 N. For the considered loading, an average number of cycles to failure of $N_f^{exp} = 5339$ has been measured on the sample submitted to a loading frequency of 1 Hz. The corresponding accumulated plastic strain increment $\Delta p = 0.0211$ has been obtained from the FE simulation of the measured total strain amplitude. When the sample is facing the same loading at 4 Hz, a plastic strain amplitude $\Delta p = 0.0192$ is obtained and an average number of cycles to failure of $N_f^{exp} = 6875$ is measured. The difference in the strain amplitude can be explained by the strain rate sensitivity (viscous behavior) of the substrate. A faster solicitation results in a stiffer response of the substrate and thus a lower applied strain amplitude for a given maximum force. These different results are nevertheless consistent regarding the Coffin-Manson relation with the identified parameters on tests at 1 Hz. Indeed, with the identified law (9), for an accumulated plastic strain increment $\Delta p = 0.0192$, the predicted N_f is 6911 cycles. This is consistent with the experimental measurement $N_f^{exp} = 6875$ (see Fig. 9a). Therefore, the Coffin-Manson law is valid for the investigated range of applied strain rate.

Samples have been manufactured from materials adopted in the PCB industry. Therefore, the results can be used for predictions of the fatigue life of flexible PCBs. However, the present results can not be adopted for the prediction of the fatigue life of PTHs in multilayer PCBs, as the behavior of the electrodeposited copper is significantly varied, due to different processing routes and microstructures.

4. Lifetime estimation of a flexible printed circuit board under cyclic folding

In the previous sections, the elastic-plastic and fatigue behaviors of a rolled annealed copper foil have been identified. This type of copper is often used in the flexible PCB industry and the mechanical properties previously identified can be used for predictive simulations, in order to prevent early failure in considered structures.

As an example of application, a simple structure composed of copper laying on a substrate has been selected here. This structure is connected at both ends to rigid devices. One of the devices is rotated with respect to the other, leading to the bending of the flexible structure. The reverse bending stage is also considered. For illustration purpose, we consider a structure which is 20 mm long. The polyimide substrate is 71.38 µm thick and the copper layer present only on the top surface of the substrate is 18.15 µm thick. Perfect bonding of the interface is assumed. The width of the structure is assumed large so that a plane strain 2D finite element simulation is carried out with the commercial software Abaqus. The flexible structure is facing 10 alternate folding/unfolding with an angular amplitude of

Coffin-Manson model parameter	ε_f	c
Identified value	1.606	-0.537

Table 3: Identified parameters for the Coffin-Manson model, describing the low-cycle fatigue behavior of the particular rolled annealed copper foil studied (18.15 µm thick on a 71.4 µm thick polyimide substrate). The values can broadly vary for different configurations (copper grade, thickness, substrate, etc.).

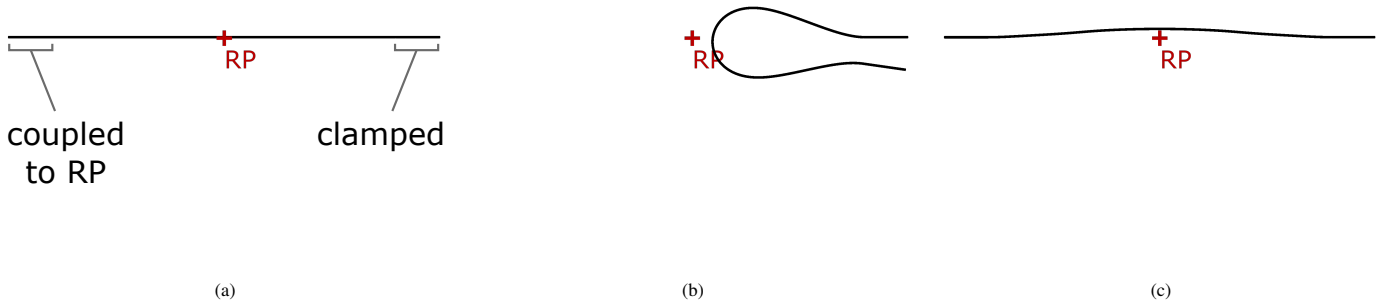

(a) (b) (c)

Figure 10: Simulation of folding/unfolding process of a flexible PCB. Successive views, from (a) initial configuration, (b) folded configuration, to (c) unfolded configuration. This sequence of images depicts the first cycle for the considered loading.

3 rad. The geometrical configuration of the flexible PCB during the full cycle is presented in Fig. 10 with 3 intermediate steps. Fig. 10a presents the initial configuration. Fig. 10b presents the configuration where the flexible PCB is folded (angular amplitude of 3 rad). The maximum stress and strain are observed in this configuration. Fig. 10c presents the shape of the flexible PCB after unfolding. The specimen is not flat anymore because of plasticity development in the top layer made of copper. Note that during the subsequent sequences of folding/unfolding, the deviation from a planar shape is increasing with the cycles.

From the numerical point of view, in order to account for the possible connection of the flexible PCB to rigid boards or devices, the bottom nodes on the right end of the structures are clamped along a 2 mm distance (see Fig. 10a). The bottom nodes along a 2 mm distance on the left end have all been coupled to a reference point denoted RP in Fig. 10. A rotation from zero to three radians, and back to zero has been imposed to this reference point to generate the folding and unfolding process.

The substrate behavior, representative of polyimide, is assumed isotropic linear elastic. Young's modulus and Poisson's ratio are respectively $E = 8\,\mathrm{GPa}$ and $\nu = 0.28$. The rolled annealed copper, layered on the top surface of the substrate, has an elastic-plastic behavior represented with the combined hardening model described in Section 3.1. The material parameters can be found in Table 2.

The considered structure is meshed with 8-node biquadratic plane strain quadrilateral elements with reduced integration (named CPER8 elements in Abaqus software). A mesh convergence study was carried out. The reference mesh presents 4 elements in the film thickness and 10 000 elements in total, see Fig. 11. By considering a denser mesh (8 elements in the film thickness, 40 000 elements in total), no difference (less than 0.02 % relative difference) was observed in the evolution of the accumulated plastic strain during cycles. As a consequence, the mesh with 10 000 elements was adopted in the following.

After the first folding stage (Fig. 10b), the maximum straining of copper and substrate is observed in the middle of the structure (see Fig. 11a). Next, only results in this cross-section will be discussed. The internal (bottom) surface made of substrate is facing longitudinal compressive stress, whereas the external (top) copper surface is under tensile stress. For the sake of clarity, a local coordinate system has been created. The x-direction is locally oriented along the length of the structure, the z-direction corresponds to the through-thickness direction and the y-direction is normal to the considered plane (see Fig. 11).

Because of bending, the stress component σ_{xx} in the copper layer reaches its maximum value at the outer surface (at the origin of the coordinate system in Fig. 11a). At the end of the bending operation (after a rotation of 3 rad) $\sigma_{xx}^{max} = 145.7\,\mathrm{MPa}$. The value of σ_{yy}^{max} reaches 72.3 MPa. The development of σ_{yy} can be explained mostly because of the plane-strain assumption (see for example the work of Simlissi et al. [30]). The magnitude of the stress components σ_{zz} and σ_{xz} remain lower than 0.5 MPa at any time. It is noticed that the stress-strain response stabilizes after four cycles only (results not presented here). The accumulated plastic strain increment Δp per cycle is stationary after a few cycles and its stabilized value is $\Delta p = 0.058$. According to Eq. (9) with the parameters identified in Section 2.2, the corresponding low-cycle fatigue life is estimated to $N_f = 882$ cycles. Note that when the sample is shorter or thicker, the bending process is more severe and the number of cycles before failure could be strongly reduced.

5. Conclusion

The development of predictive capability by numerical simulations of PCB reliability needs a proper material characterization. In the present work, we concentrate on copper and investigate the mechanical response of thin copper foils under cyclic loading. A configuration representative of flexible printed circuits is selected: Rolled Annealed (RA) copper film layered on

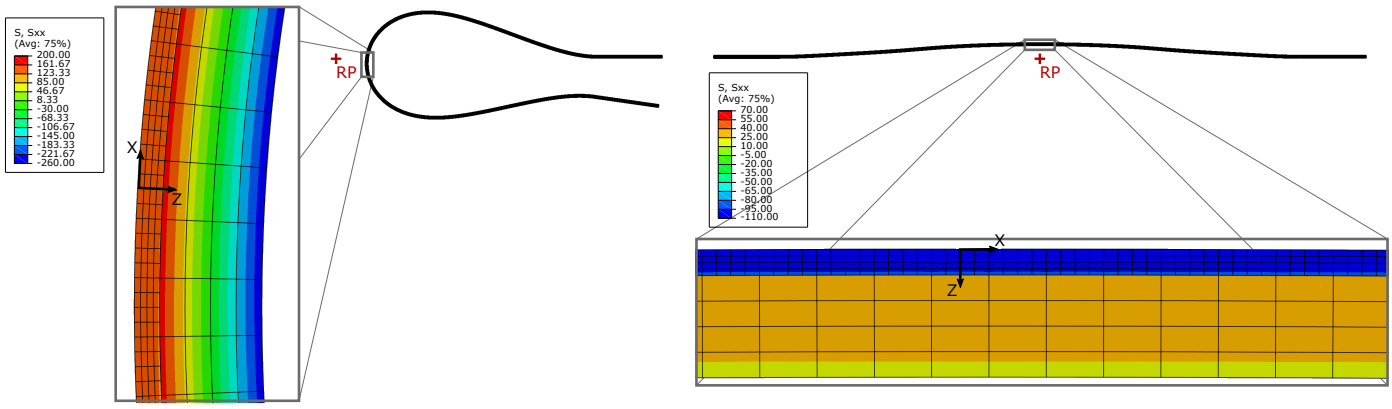

Figure 11: Results of cyclic folding/unfolding simulation of the flexible structure. Map of the longitudinal stress component σ_{xx} (in MPa) (a) at the end of the first folding. Positive longitudinal stresses are observed within the rolled annealed copper layer. The maximum stress reaches $145.7\,\mathrm{MPa}$. (b) after unfolding. Due to plasticity development during folding, the sample is not flat. The copper layer experiences almost homogeneous negative longitudinal stress, around $-100\,\mathrm{MPa}$. The longitudinal stresses are expressed in the local coordinate system shown in the figures.

a polyimide substrate.

Two series of experiments are conducted on the same materials to capture two important features: the cyclic stress-strain response and the fatigue life of copper. From loading-unloading on the composite sample (polyimide substrate + RA copper), it is demonstrated that a clear kinematic hardening develops in copper during cycles. Therefore, the constitutive response is identified via the classical Lemaitre-Chaboche model, which integrates a combined isotropic and kinematic hardening.

To capture the fatigue behavior of copper, a specific sample design is proposed with twelve copper tracks. The number of cycles to failure of each track is captured by monitoring the electrical resistance of copper along the test. Owing to the specific sample design (twelve tracks), the variability in number of cycles to failure is quantified with a limited number of tests. This is one of the main advantages of the proposed sample. As the copper response is known, a Coffin-Manson model is identified which relates the failure to the increment of accumulated plastic strain during the stabilized cycle.

Finally, the experimental data and corresponding modelings obtained in this paper are transferred to a simulation of alternate bending of a flexible PCB. An estimate of the fatigue life is provided.

As both the constitutive behavior and the fatigue life are provided in the same work, this information can be adopted with great confidence for the reliability assessment of flexible printed circuits. The important advantage of developing samples with combination of material really used in the industry is that data can be directly used for this specific design. The next step is the validation of the material models on real flexible printed circuits and will be carried out in a future work. The proposed methodology could be adopted for other configurations such as FR4 + electrodeposited copper.

All data are obtained at room temperature, so with the proposed work, we can assess the reliability of flexible circuits, strained at ambient temperature. For PCBs operating under thermal loads, one needs to perform similar tests at various temperatures. This investigation will also be conducted in a near future.

Acknowledgments

The authors thank the support of Région Grand Est with the grant “soutien aux jeunes chercheurs” for G. Girard. The financial support of Metz Métropole and Département de la Moselle is acknowledged as well as those of CIMULEC, SYSTRONIC and CSI SUD OUEST through the NIT foundation.

References

[1] G. Girard, M. Jrad, S. Bahi, M. Martiny, S. Mercier, L. Bodin, D. Nevo, S. Dareys, Experimental and numerical characterization of thin woven composites used in printed circuit boards for high frequency applications, Composite Structures 193 (2018) 140 – 153.

[2] Y. Wang, H. Wang, F. Liu, X. Wu, J. Xu, H. Cui, Y. Wu, R. Xue, C. Tian, B. Zheng, W. Yao, Flexible printed circuit board based on graphene/polyimide composites with excellent thermal conductivity and sandwich structure, Composites Part A: Applied Science and Manufacturing 138 (2020) 106075.

[3] K. Weinberg, W. H. Müller, A strategy for damage assessment of thermally stressed copper vias in microelectronic printed circuit boards, Microelectronics Reliability 48 (1) (2008) 68 – 82.

[4] K. Fellner, T. Antretter, P. F. Fuchs, Q. Toa, Numerical simulation of the electrical performance of printed circuit boards under cyclic thermal loads, Microelectronics Reliability 62 (2016) 148–155.

[5] S. Q. Huang, K. C. Yung, B. Sun, A finite element model and experimental analysis of PTH reliability in rigid-flex printed circuits using the taguchi method, International Journal of Fatigue 40 (2012) 84–96.

[6] A. Salahouelhadj, M. Martiny, S. Mercier, L. Bodin, D. Manteigas, B. Stephan, Reliability of thermally stressed rigid–flex printed circuit boards for high density interconnect applications, Microelectronics Reliability 54 (1) (2014) 204 – 213.

[7] H. D. Merchant, M. G. Minor, C. S. J., L. D. T., 18 μm electrodeposited copper foil for flex fatigue applications, Circuit World 25 (1) (1998) 38 – 46.

[8] H. D. Merchant, M. G. Minor, Y. L. Liu, Mechanical fatigue of thin copper foil, Journal of Electronic Materials 28 (9) (1999) 998 – 1007.

[9] L. F. J. Coffin, A study of the effects of cyclic thermal stresses on a ductile meta, Transactions of the ASME 76 (1954) 931–950.

[10] S. S. Manson, Fatigue: A complex subject—some simple approximations, Experimental Mechanics 5 (4) (1965) 193–226.

[11] K. Watanabe, Y. Kariya, N. Yajima, K. Obinata, Y. Hiroshima, S. Kikuchi, A. Matsui, H. Shimizu, Low-cycle fatigue testing and thermal fatigue life prediction of electroplated copper thin film for through hole via, Microelectronics Reliability 82 (2018) 20 – 27.
[12] F. Su, R. Mao, J. Xiong, K. Zhou, Z. Zhang, J. Shao, C. Xie, On thermo-mechanical reliability of plated-through-hole (PTH), Microelectronics Reliability 52 (2012) 1189–1196.
[13] D.-J. Lee, J.-S. Lee, T.-W. Kim, S.-Y. Lee, Y.-B. Park, Y.-C. Joo, B.-J. Kim, Effect of the thermal annealing on the stretchability and fatigue failure of the copper film on the polymer substrate, Journal of Electronic Materials 48 (2019) 4582 – 4588.
[14] D. Beck, D. Susan, N. Sorensen, G. Thayer, Fatigue behavior of thin cu foils and cu/kapton flexible circuits, Tech. Rep. SAND2008-4293C (February 2008).
[15] Y. Xiang, X. Chen, J. J. Vlassak, The mechanical properties of electroplated cu thin films measured by means of the bulge test technique, MRS Proceedings 695 (2001) L4.9.1.
[16] R. Dudek, R. Döring, M. Hildebrandt, S. Rzepka, S. Stegmeier, S. Kiefl, V. Sommer, G. Mitic, K. Weidner, Analyses of thermo-mechanical reliability issues for power modules designed in planar technology, EuroSimE.
[17] O. Kraft, R. Schwaiger, P. Wellner, Fatigue in thin films: lifetime and damage formation, Materials Science and Engineering: A 319-321 (2001) 919 – 923.
[18] O. Kraft, P. Wellner, M. Hommel, R. Schwaiger, E. Arzt, Fatigue behavior of polycrystalline thin copper films, Zeitschrift für Metallkunde 93 (2002) 392–400.
[19] Y. Ono, S. Morito, Investigation into early fatigue damage in electrodeposited copper, International Journal of Fatigue 54 (2013) 7–16.
[20] R. Mönig, R. R. Keller, C. A. Volkert, Thermal fatigue testing of thin metal films, Review of Scientific Instruments 75 (11) (2004) 4997–5004.
[21] A. Wimmer, A. Leitner, T. Detzel, W. Robl, W. Heinz, R. Pippan, G. Dehm, Damage evolution during cyclic tension–tension loading of micron-sized cu lines, Acta Materialia 67 (2014) 297 – 307.
[22] K. Fellner, P. Fuchs, G. Pinter, T. Antretter, T. Krivec, Method development for the cyclic characterization of thin copper layers for pcb applications, Circuit World 40 (2014) 53–60.
[23] J.-L. Chaboche, Time-independant constitutive theories for cyclic plasticity, International Journal of Plasticity 2 (1986) 149–188.
[24] J.-L. Chaboche, On some modifications of kinematic hardening to improve the description of ratchetting effects, International Journal of Plasticity 7 (1991) 661–678.
[25] K. Fellner, T. Antretter, P. F. Fuchs, T. Pélisset, Cyclic mechanical behavior of thin layers of copper: A theoretical and numerical study, EuroSimE (2015) 1–9.
[26] G. Simons, C. Weippert, J. Dual, J. Villain, Size effects in tensile testing of thin cold rolled and annealed cu foils, Materials Science and Engineering: A 416 (1) (2006) 290 – 299.
[27] Institute for Interconnecting and Packaging Electronic Circuits, Flexural Fatigue and Ductility, Flexible Printed Wiring (March 1991).
[28] F. Macionczyk, Brückner, Tensile testing of alcu thin films on polyimide foils, Journal of Applied Physics 86 (1999) 4922–4929.
[29] S. Su, F. J. Akkara, R. Thaper, A. Alkhazali, M. Hamasha, S. Hamasha, A State-of-the-Art Review of Fatigue Life Prediction Models for Solder Joint, Journal of Electronic Packaging 141 (4).
[30] E. Simlissi, M. Martiny, S. Mercier, S. Bahi, L. Bodin, Elastic–plastic analysis of the peel test for ductile thin film presenting a saturation of the yield stress, International Journal of Fracture 220 (1) (2019) 1 – 16.